

## 645 A *Lo-Hi* benchmark

646 *Lo-Hi* is a practical ML drug discovery benchmark, comprising two tasks: Hit Identification (Hi) and  
647 Lead Optimization (Lo). Hi corresponds to a binary classification problem, wherein the goal is to  
648 identify novel hits that differ significantly from the training dataset [10, 11, 16, 27, 28]. This is why  
649 there are no molecules in the test set with ECFP4 Tanimoto similarity exceeding 0.4 to the training  
650 set. Models are compared using the PR AUC metric.

651 Lo is a ranking problem that pertains to optimizing molecules or guiding molecular generative models.  
652 The test set consists of clusters of similar molecules that are largely dissimilar from the training  
653 set, except for one molecule representing a known hit. The task involves ranking the activity of the  
654 molecules within clusters, hence we use mean intercluster Spearman correlation to evaluate models.  
655 To ensure that the variation in intracluster activity stems from actual differences in activity rather than  
656 random noise, we selected clusters demonstrating high variation, as detailed in Appendix B and C.

657 The datasets each consist of three folds. We advise using the first fold for hyperparameter selection,  
658 and then applying these hyperparameters across all folds.

659 Datasets are released under the MIT license. Authors bear all responsibility in case of violation of  
660 rights. Datasets are small .csv files, that is why we are going to keep them in the public GitHub  
661 repository. Reviewers can find datasets in data folder.

662 In this section, we provide further information regarding the datasets and preprocessing steps. The  
663 size and diversity of the original datasets are displayed in Table 3.

Table 3: Original datasets

Dataset	Size	#Circles [69] (0.5)	Active fraction
DRD2 (Ki)	8482	837	0.731
HIV	41127	19222	0.035
KDR (IC50)	8826	791	0.643
Sol	2173	1763	0.216
KCNH2 (IC50)	11159	2128	NA

### 664 A.1 Data preprocessing

665 We began by canonicalizing all SMILES using RDKit 2022.9.5.

666 For DRD2-Hi, DRD2-Lo, KDR-Hi, KDR-Lo and KCNH2-Lo we utilized data from the  
667 ChEMBL30 [74] database. We collected data points that measured Ki (for DRD2) and  
668 IC50 (for KCNH2 and KDR) with `confidence_score`  $\geq 6$ . We selected those for  
669 which `standard_units` were in "nM". We converted `standard_value` to logarithmic scale,  
670 also known as `pChEMBL`([https://chembl.gitbook.io/chembl-interface-documentation/  
671 frequently-asked-questions/chembl-data-questions#what-is-pchembl](https://chembl.gitbook.io/chembl-interface-documentation/frequently-asked-questions/chembl-data-questions#what-is-pchembl)).

672 For binary DRD2-Hi and KDR-Hi we binarized the data such that log activity values greater than 6  
673 (which is  $< 10$   $\mu$ M) were designated as 1, and all others as 0. We removed any ambiguous data  
674 points (e.g. with `standard_relation` of "<" and an activity value more than 10  $\mu$ M, because  
675 those could not be binarized reliably). Following this, we selected data points with identical SMILES,  
676 discarding any with differing binarized activities.

677 For the continuous DRD2-Lo, KDR-Lo and KCNH2-Lo datasets, we selected data points that had  
678 `standard_relation` of '=' and a log activity value greater than 5 but less than 9. We selected data  
679 points with identical SMILES, discarding any with activity differences greater than 1.0. For the  
680 remaining data, we took the median of each group.

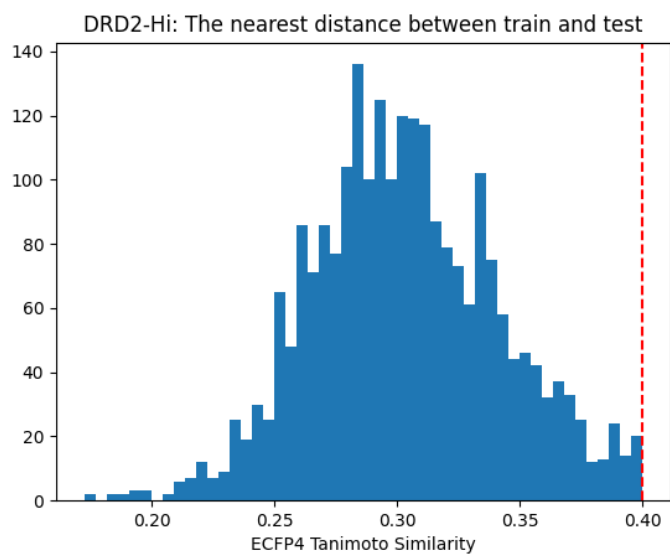


Figure 4: DRD2-Hi: Fold 1

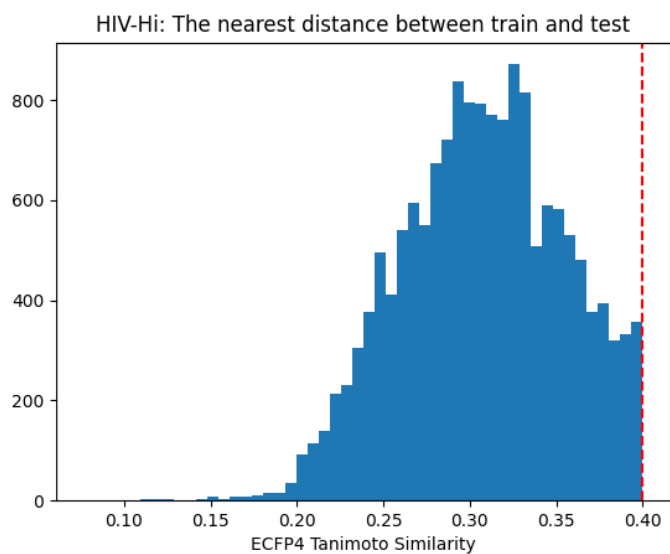


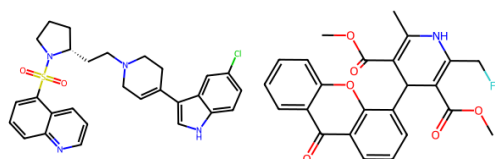
Figure 5: HIV-Hi: Fold 1

Table 4: Hi folds

Dataset	Train 1	Test 1	Train 2	Test 2	Train 3	Test 3
DRD2-Hi	2385	1190	2381	1194	2384	1191
HIV-Hi	15696	7847	15695	7848	15695	7848
KDR-Hi	500	3116	500	3125	500	2285
So1-Hi	1442	721	1442	721	1442	721

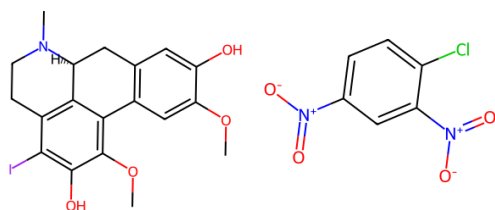
Table 5: Lo folds

Dataset	Train 1	Test 1	Train 2	Test 2	Train 3	Test 3
DRD2-Lo	2206	267	2128	267	2257	262
KCNH2-Lo	3313	406	3313	406	3313	406
KDR-Lo	500	437	500	520	500	417



DRD2-Hi: Fold 1 train

HIV-Hi: Fold 1 train



DRD2-Hi: Fold 1 test

HIV-Hi: Fold 1 test

Figure 6: The most similar pairs of molecules between train and test.

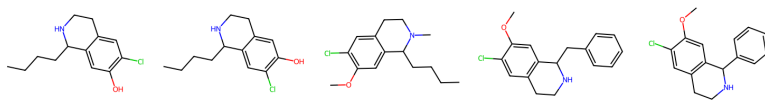


Figure 7: Example of Lo cluster in DRD2-Lo

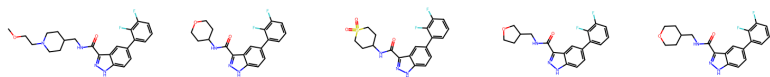


Figure 8: Example of Lo cluster in KCNH2-Lo

## 681 B Lo dataset is not just noise

682 Experimental data inherently contain noise. Consequently, selecting similar molecules may result in  
683 clusters that possess such a small variation that it could be solely attributable to experimental noise,  
684 thereby invalidating the Lo task. This potential issue underlines the importance of ascertaining that  
685 the clusters exhibit a significant signal to ensure the validity of the task.

686 As reported [87], the standard deviation for the same ligand-protein pair’s pIC50 is  $\sigma_{pIC50} \approx 0.20$   
687 when measured in the same laboratory, and  $\sigma_{pIC50} \approx 0.68$  in the ChEMBL database. In similar  
688 work [88] standard deviation for ChEMBL pKi was found to be  $\sigma_{pKi} \approx 0.56$ . Therefore, based on  
689 these findings, we opted to select only those clusters that displayed a standard deviation exceeding  
690 0.70 for pIC50 and more than 0.60 for pKi. These selection criteria enhance the confidence in the  
691 validity of the Lo task by prioritizing clusters with significant intracluster variation.

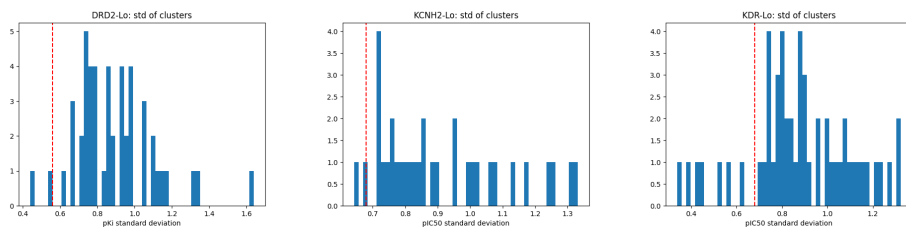


Figure 9: Within cluster variability is higher than noise standard deviation.

## 692 C Lo algorithm

693 The Python implementation can be found in `code/splits.py`.

---

### Algorithm 1 Get Lo Split

**Input:** List of molecular SMILES  $S$ , similarity threshold  $t$ , minimum cluster size  $m$ , maximum number of clusters  $M$ , activity values  $V$ , standard deviation threshold  $std_t$

**Output:** List of SMILES clusters  $C$ , list of remaining training SMILES  $train\_S$

```
1: procedure GETLOSPLIT( $S, t, m, M, V, std_t$ )
2:    $C, train\_S \leftarrow$  SELECTDISTINCTCLUSTERS( $S, t, m, M, V, std_t$ )
3:   for each  $cluster$  in  $C$  do
4:     Move central molecule from  $cluster$  to  $train\_S$ 
5:   end for
6:   return  $C, train\_S$ 
7: end procedure
```

---

---

**Algorithm 2** Select Distinct Clusters

---

**Input:** List of molecular SMILES  $S$ , similarity threshold  $t$ , minimum cluster size  $m$ , maximum number of clusters  $M$ , activity values  $V$ , standard deviation threshold  $std_t$

**Output:** List of SMILES clusters  $C$ , list of the rest training SMILES  $train\_S$

```
1: function SELECTDISTINCTCLUSTERS( $S, t, m, M, V, std_t$ )
2:    $train\_S \leftarrow S$ 
3:   Initialize list  $C$  as empty
4:   while length of  $C < M$  do
5:     Compute fingerprints  $F$  from SMILES in  $train\_S$ 
6:     Compute total number of neighbors  $N$  for each fingerprint in  $F$ 
7:     Compute  $STD$  standard deviation of  $V$  of neighbors for each fingerprint in  $F$ 
8:     Set  $central\_idx$  to None
9:     Set  $least\_neighbors$  to  $\max(N)$ 
10:    for each  $idx$  in  $0..|train\_S|$  do ▷ Find the smallest cluster that meets criteria
11:      if  $N[idx] > m$  and  $STD[idx] > std_t$  and  $N[idx] < least\_neighbors$  then
12:         $central\_idx \leftarrow idx$ 
13:         $least\_neighbors \leftarrow N[idx]$ 
14:      end if
15:    end for
16:    if  $central\_idx$  is None then ▷ Exit if there are no more clusters that meet criteria
17:      break
18:    end if
19:    Add  $central\_idx$  molecule and its neighbors to list of clusters  $C$ 
20:    Remove the cluster and its neighbors from  $train\_S$ 
21:  end while
22:  return  $C, train\_S$ 
23: end function
```

---

694 **D Additional benchmarks analysis**

695 Distribution of Tanimoto Similarity between the nearest molecules between train and test.

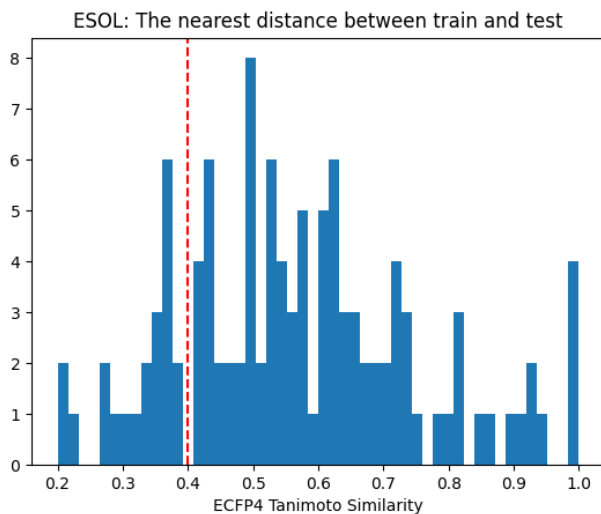


Figure 10: ESOL

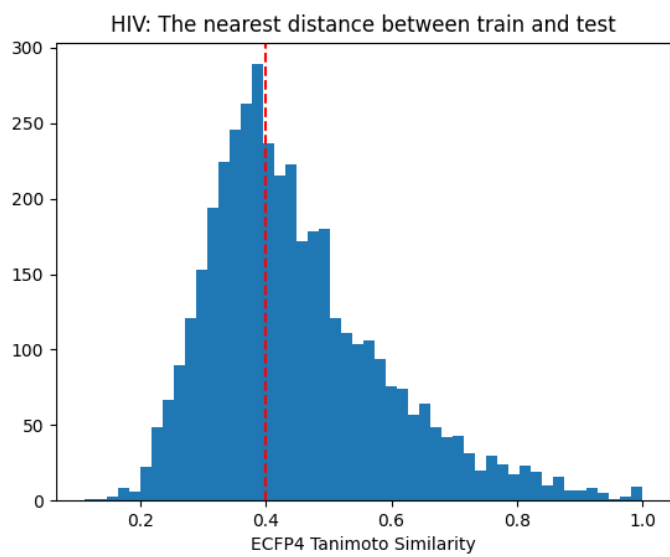


Figure 11: HIV

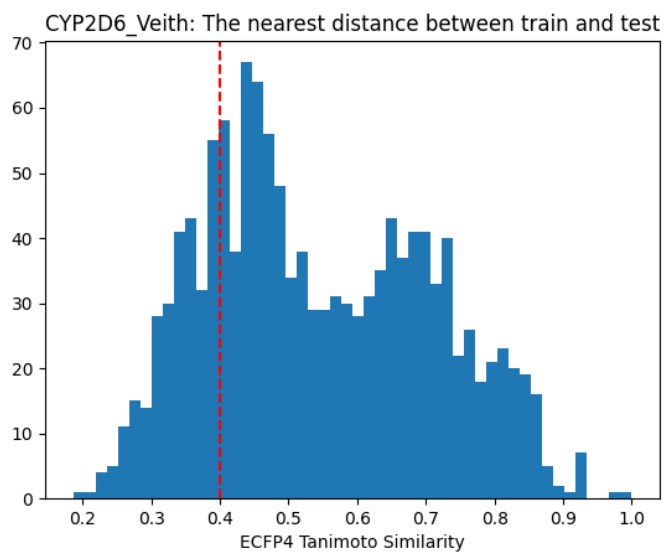


Figure 12: TDC

696 We additionally analyzed other ligand-based MoleculeNet datasets.

Table 6: Fraction of test molecules in various MoleculeNet datasets with a Tanimoto similarity  $>0.4$  to the train set using ECFP4 fingerprints.

Dataset	Fraction of Test Molecules Similar to Train Set
QM7	0.93
QM8	0.98
QM9	0.99
FreeSolv	0.8
Lipophilicity	0.67
PCBA	$>0.93$
MUV	0.96
BACE	0.77
Tox21	0.52
SIDER	0.48

## 697 E Graph coarsening algorithm

698 The Python implementation can be found in `code/min_vertex_k_cut.py`. We are planning to  
699 release it as a pip package.

---

### Algorithm 3 Calculate Neighbors

---

**Input:** Graph  $G = (V, E)$ , similarity threshold  $\theta$

**Output:** List of tuples  $n\_neighbors$

```
1: function CALCULATENEIGHBORS( $G, \theta$ )
2:   Initialize list  $n\_neighbors$  as empty
3:   for each node  $v$  in  $V$  do
4:     Initialize  $total\_neighbors$  as 0
5:     for each edge  $e$  incident on node  $v$  do
6:       if  $e['similarity'] > \theta$  then
7:          $total\_neighbors \leftarrow total\_neighbors + 1$ 
8:       end if
9:     end for
10:    Append  $(total\_neighbors, \text{index of } v)$  to  $n\_neighbors$ 
11:  end for
12:  return  $n\_neighbors$ 
13: end function
```

---

---

**Algorithm 4** Cluster Nodes

---

**Input:** Sorted list  $n\_neighbors$ , Graph  $G = (V, E)$ , similarity threshold  $\theta$

**Output:** Cluster assignment  $node\_to\_cluster$ , number of clusters  $total\_clusters$

```
1: function CLUSTERNODES( $n\_neighbors, G, \theta$ )
2:   Initialize array  $node\_to\_cluster$  of size  $|V|$  as  $-1$ 
3:   Initialize  $total\_clusters$  as 1
4:   for each tuple  $(count, node)$  in  $n\_neighbors$  do
5:     if  $node\_to\_cluster[node] = -1$  then
6:        $node\_to\_cluster[node] \leftarrow total\_clusters$  ▷ Assign new cluster
7:       for each edge  $e$  incident on node  $node$  do
8:         if  $e[‘similarity’] > \theta$  then
9:            $adjacent\_node \leftarrow e[1]$ 
10:          if  $node\_to\_cluster[adjacent\_node] = -1$  then
11:             $node\_to\_cluster[adjacent\_node] \leftarrow total\_clusters$ 
12:          end if
13:        end if
14:      end for
15:       $total\_clusters \leftarrow total\_clusters + 1$ 
16:    end if
17:  end for
18:  return  $node\_to\_cluster, total\_clusters$ 
19: end function
```

---

---

**Algorithm 5** Build Coarse Graph

---

**Input:** Cluster assignment  $node\_to\_cluster$ , number of clusters  $total\_clusters$ , Graph  $G = (V, E)$

**Output:** Coarsened Graph  $G_{coarse}$

```
1: function BUILDCOARSEGRAPH( $node\_to\_cluster, total\_clusters, G$ )
2:   Compute  $clusters\_size$ , count of each unique element in  $node\_to\_cluster$ 
3:   Initialize  $G_{coarse}$  as an empty graph
4:   for  $cluster$  in 0 to  $total\_clusters - 1$  do ▷ Add nodes
5:     Add node  $cluster$  with weight  $clusters\_size[cluster]$  to  $G_{coarse}$ 
6:   end for
7:   for  $cluster$  in 0 to  $total\_clusters - 1$  do ▷ Add edges
8:     Initialize  $connected\_clusters$  as an empty set
9:     Get nodes of  $cluster$  as  $this\_cluster\_indices$  where  $node\_to\_cluster$  equals  $cluster$ 
10:    for each  $node$  in  $this\_cluster\_indices$  do
11:      for each edge  $e$  incident on node  $node$  do
12:        Add  $node\_to\_cluster[e[1]]$  to  $connected\_clusters$ 
13:      end for
14:    end for
15:    for each  $connected\_cluster$  in  $connected\_clusters$  do
16:      Add edge from  $cluster$  to  $connected\_cluster$  in  $G_{coarse}$ 
17:    end for
18:  end for
19:  return  $G_{coarse}$ 
20: end function
```

---

---

**Algorithm 6** Main Procedure

---

**Input:** Graph  $G = (V, E)$ , similarity threshold  $\theta$

**Output:** Coarsened graph  $G_{coarse}$

```
1: procedure COARSEGRAPH( $G, \theta$ )
2:    $n\_neighbors \leftarrow CALCULATENEIGHBORS(G, \theta)$ 
3:   Sort  $n\_neighbors$  in descending order of first element of each tuple
4:    $node\_to\_cluster, total\_clusters \leftarrow CLUSTERNODES(n\_neighbors, G, \theta)$ 
5:    $G_{coarse} \leftarrow BUILDCOARSEGRAPH(node\_to\_cluster, total\_clusters, G)$ 
6:   return  $G_{coarse}$ 
7: end procedure
```

---

## 700 F Hi-split predicts virtual screening hit rate better than scaffold split

701 For effective virtual screening, predicting experimental outcomes prior to experimentation is  
702 paramount. In this study, we compare the predictive performance of the novel Hi-split approach  
703 with the traditional scaffold split method under a Hit Identification scenario. Following existing  
704 literature [10, 11, 16, 27, 28], we simulate testing on novel molecules with an ECFP4 Tanimoto  
705 similarity of  $\leq 0.4$  to the training set. The dataset is partitioned using both splitting methods to  
706 form separate training and validation sets for hyperparameter selection. Hyperparameter search is  
707 performed for gradient boosting on ECFP4 fingerprints, identified as the most efficient Hi model that  
708 facilitates quick training.

709 After selecting the optimal hyperparameters, performance metrics are computed on the validation set.  
710 Subsequently, the model is retrained on the combined training and validation sets, and performance  
711 metrics for the hold-out test set are calculated to simulate the application of a trained model in virtual  
712 screening. The results are summarized in Table 7.

Table 7: Hi-split vs scaffold split

Dataset	Validation	Test
DRD2-Hi (Hi split)	0.603	<b>0.677</b>
DRD2-Hi (Scaffold split)	0.872	0.663
HIV-Hi (Hi split)	0.069	<b>0.084</b>
HIV-Hi (Scaffold split)	0.189	0.078

713 The Hi-split method demonstrates superior predictive performance for virtual screening hit rate  
714 compared to the scaffold split method, which is over-optimistic in the Hit Identification scenario. It  
715 also improved the test evaluation metric, although the difference is not substantial. The improved  
716 performance of the Hi-split may be attributed to the selection of more regularized models.

## 717 G Novelty consensus analysis

718 We have reproduced the work presented in [43] using binary ECFP4 fingerprints, as calculated by  
719 RDKit version 2022.9.5. The results can be found in Figure 13. For this particular work, we selected  
720 0.40 as the novelty threshold.

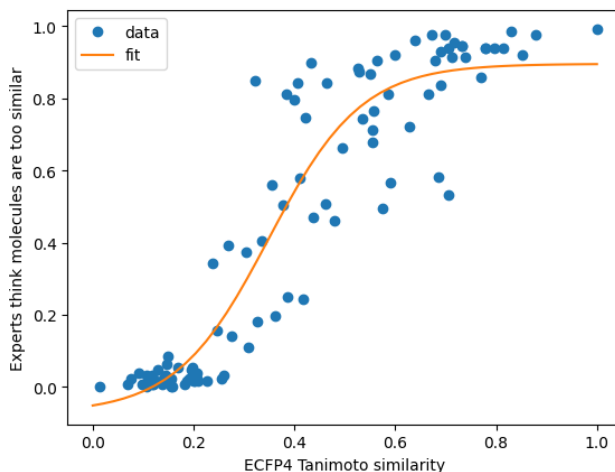


Figure 13: Sigmoid fit to [43] data

## 721 H Hyperparameter optimization

722 We used random or grid search to optimize hyperparameters for all models except for the Graphormer,  
723 which was too slow for meticulous hyperparameter search. Here we provide optimization parameters  
724 and additional commentary on the training.

725 We utilized a single NVIDIA RTX 2070 SUPER with CUDA 11.7 and calculated binary 1024 ECFP4  
726 and MACCS fingerprints using RDKit 2022.9.5.

### 727 H.1 Dummy baseline

728 Always predicts the same constant value.

### 729 H.2 KNN

730 We used `scipy.spatial.distance.jaccard` as the distance metric, as it outperformed the stan-  
731 dard Euclidian distance in our use case. We used grid search with all combinations of parameters.  
732 For ECFP4 it was:

```
733     params = {  
734         'n_neighbors': [3, 5, 7, 10],  
735         'weights': ['uniform', 'distance'],  
736     }
```

737 and for MACCS:

```
738     params = {  
739         'n_neighbors': [3, 5, 7, 10, 12, 15],  
740         'weights': ['uniform', 'distance'],  
741     }
```

### 742 H.3 Gradient Boosting

743 We used 30 iterations of random search with these parameters:

```
744     params = {  
745         'n_estimators': [10, 50, 100, 150, 200, 250, 500],  
746         'learning_rate': [0.01, 0.1, 0.3, 0.5, 0.7, 1.0],  
747         'subsample': [0.4, 0.7, 0.9, 1.0],  
748         'min_samples_split': [2, 3, 5, 7],  
749         'min_samples_leaf': [1, 3, 5],  
750         'max_depth': [2, 3, 4],  
751         'max_features': [None, 'sqrt']  
752     }
```

### 753 H.4 SVM

754 We used grid search with these parameters:

```
755     params = {  
756         'C': [0.1, 0.5, 1.0, 2.0, 5.0],  
757     }
```

### 758 H.5 MLP

759 We implemented a feed-forward neural network using Pytorch 2.0.0+cu117 and Pytorch Lightning  
760 2.0.2. It consisted of several feed-forward layers with optional dropout layers. We used early stopping

761 to prevent overfitting with patience 20 for the Hi tasks, and 10 for the Lo tasks. We used learning  
762 rate 0.01. We used batch size 32. We conducted 30 iterations of random search. For ECFP4 we used  
763 these parameters:

```
764     param_dict = {  
765         'layers': [  
766             [1024, 32, 32],  
767             [1024, 16, 16],  
768             [1024, 32],  
769             [1024, 8, 4],  
770             [1024, 4]  
771         ],  
772         'dropout': [0.0, 0.0, 0.2, 0.4, 0.6],  
773         'l2': [0.0, 0.0, 0.001, 0.005, 0.01],  
774     }
```

775 For MACCS we used these parameters:

```
776     param_dict = {  
777         'layers': [  
778             [167, 32, 32],  
779             [167, 16, 16],  
780             [167, 32],  
781             [167, 8, 4],  
782             [167, 4]  
783         ],  
784         'dropout': [0.0, 0.0, 0.2, 0.4, 0.6],  
785         'l2': [0.0, 0.0, 0.001, 0.005, 0.01],  
786     }
```

787 After the selection of the best hyperparameters, we selected a fixed number of the training epochs  
788 using early stopping. We used the same number of epochs for all the folds.

## 789 H.6 Chemprop

790 We used Chemprop 1.5.2 with rdkit features. We found the evaluation metrics to be a little better  
791 with them, but it was SOTA for Hi even without them:

```
792     '--features_generator rdkit_2d_normalized',  
793     '--no_features_scaling',
```

794 We used 20 iterations of random search with these parameters:

```
795     param_dict = {  
796         '--depth': ['3', '4', '5', '6'],  
797         '--dropout': ['0.0', '0.2', '0.3', '0.5', '0.7'],  
798         '--ffn_hidden_size': ['600', '1200', '2400', '3600'],  
799         '--ffn_num_layers': ['1', '2', '3'],  
800         '--hidden_size': ['600', '1200', '2400', '3600']  
801     }
```

802 We selected the number of epochs using only the first fold. After the hyperparameters were selected,  
803 we trained the model and did not expose it to the test data. The full command for training Chemprop  
804 for HIV-Hi dataset:

```
805     chemprop_train --data_path data/hi/hiv/train_1.csv --dataset_type classification \  
806     --save_dir checkpoints/hi/hiv/ \  

```

```
807 --config_path configs/hiv_hi \  
808 --separate_val_path data/hi/hiv/train_1.csv \  
809 --separate_test_path data/hi/hiv/train_1.csv \  
810 --metric 'prc-auc' \  
811 --epochs 40 \  
812 --features_generator rdkit_2d_normalized \  
813 --no_features_scaling
```

814 For the DRD-Hi the best hyperparameters were:

```
815 {  
816 "depth": 6,  
817 "dropout": 0.0,  
818 "ffn_hidden_size": 2400,  
819 "ffn_num_layers": 1,  
820 "hidden_size": 2400  
821 }
```

822 For the HIV-Hi the best hyperparameters were:

```
823 {  
824 "depth": 6,  
825 "dropout": 0.2,  
826 "ffn_hidden_size": 3600,  
827 "ffn_num_layers": 2,  
828 "hidden_size": 3600  
829 }
```

## 830 H.7 Graphormer

831 We used Graphormer with the last commit 77f436db46fb9013121289db670d1a763f264153. We ap-  
832 plied two fixes, that we found in issues <https://github.com/microsoft/Graphormer/issues/158#issuecomment-1500311589> and <https://github.com/microsoft/Graphormer/issues/130#issuecomment-1207316808> that solved our problems. However, we set up an  
834 in-house Graphormer some time ago and currently, it cannot be reinstalled from scratch due to  
835 multiple broken dependencies.  
836

837 We modified code to calculate and track PR AUC metrics, to add our datasets, and to evaluate trained  
838 models. We manually optimized the hyperparameters over approximately 10 iterations. We found  
839 Graphormer to be inferior to Chemprop, which is consistent with our previous experience with  
840 different datasets.

841 We faced numerous technical difficulties in executing and modifying Graphormer [80, 81] due to  
842 improper dependency pinning by the authors. We found the training to be slow, which limited our  
843 ability to optimize hyperparameters. Because of technical difficulties, we decided not to test it for the  
844 Lo task.

## 845 H.8 HIV-Hi balance

846 HIV-Hi is a highly unbalanced binary classification problem with only 3% of positive examples. Due  
847 to this imbalance, we experimented with weighted options of classical ML algorithms and manually  
848 resampled positive examples for neural networks.

849 **I Spearman distribution**

850 The test set of the Lo datasets is composed of molecular clusters. To evaluate the models, the  
851 Spearman correlation coefficient is calculated within each cluster, comparing the actual activity  
852 values to the predicted ones. The final Lo metric is the average of the Spearman coefficients across  
853 all clusters.

854 In the following, we present a histogram of Spearman coefficients for the best models across various  
855 datasets. Note that the KDR-Lo dataset is more challenging than both DRD2-Lo and KCNH2-Lo.

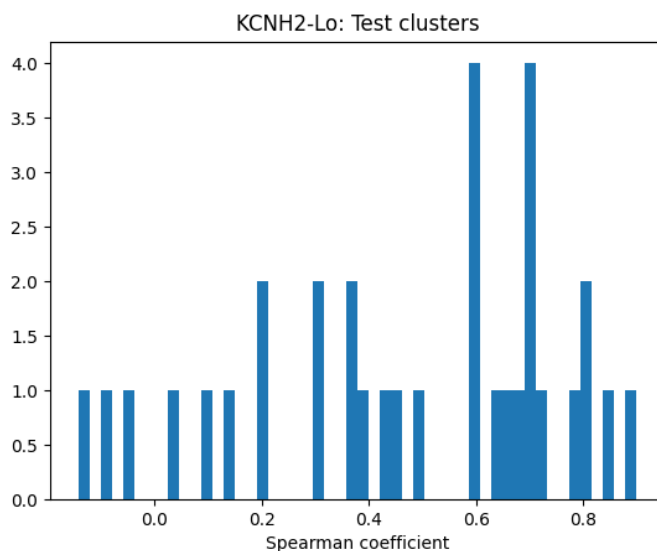


Figure 14: KCNH2-Lo Spearman coefficient distribution for SVM-ECFP4

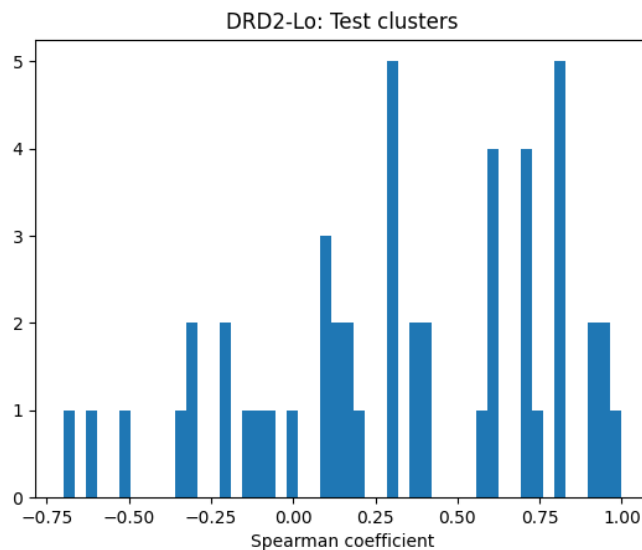


Figure 15: DRD2-Lo Spearman coefficient distribution for SVM-ECFP4

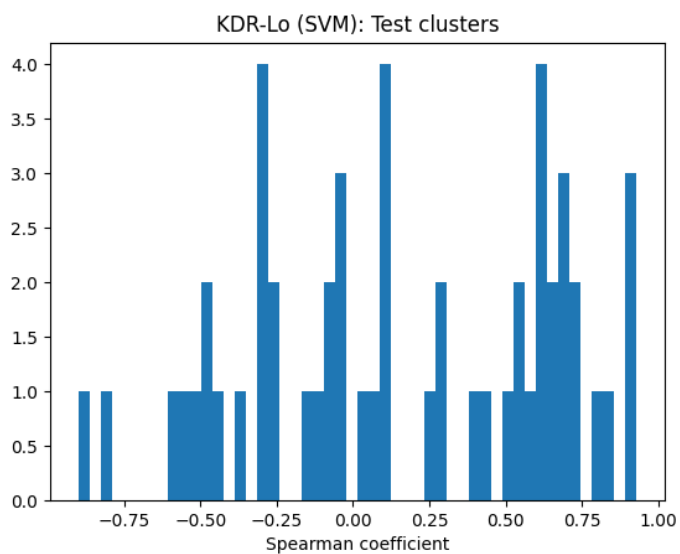


Figure 16: KDR-Lo Spearman coefficient distribution for SVM-ECFP4

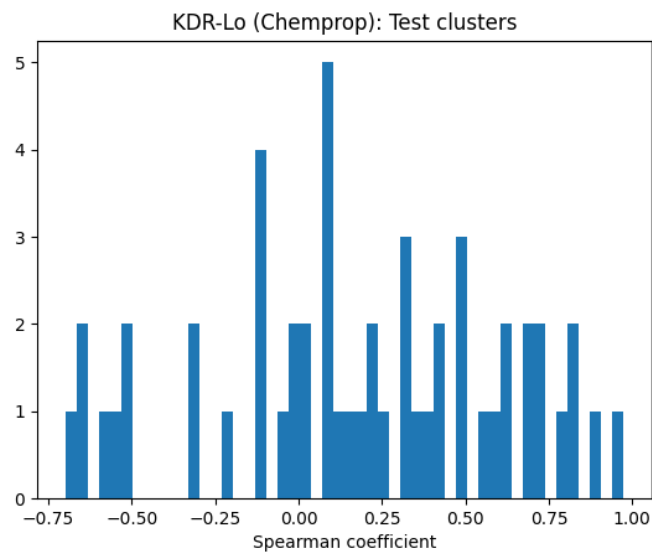


Figure 17: KDR-Lo Spearman coefficient distribution for Chemprop

## References

- 856
- 857 [1] Shu-Feng Zhou and Wei-Zhu Zhong. Drug design and discovery: principles and applications,  
858 2017.
- 859 [2] Jing Lin, Diana C Sahakian, SM De Morais, Jinghai J Xu, Robert J Polzer, and Steven M Winter.  
860 The role of absorption, distribution, metabolism, excretion and toxicity in drug discovery.  
861 *Current topics in medicinal chemistry*, 3(10):1125–1154, 2003.
- 862 [3] Sabina Podlewska and Rafał Kafel. Metstabon—online platform for metabolic stability predic-  
863 tions. *International journal of molecular sciences*, 19(4):1040, 2018.
- 864 [4] Mohsen Sharifi and Taravat Ghafourian. Estimation of biliary excretion of foreign compounds  
865 using properties of molecular structure. *The AAPS journal*, 16:65–78, 2014.
- 866 [5] Patrizia Crivori, Gabriele Cruciani, Pierre-Alain Carrupt, and Bernard Testa. Predicting blood-  
867 brain barrier permeation from three-dimensional molecular structure. *Journal of medicinal*  
868 *chemistry*, 43(11):2204–2216, 2000.
- 869 [6] Qiang Tang, Fulei Nie, Qi Zhao, and Wei Chen. A merged molecular representation deep  
870 learning method for blood–brain barrier permeability prediction. *Briefings in Bioinformatics*,  
871 23(5), 2022.
- 872 [7] Raimund Mannhold and Han Van de Waterbeemd. Substructure and whole molecule approaches  
873 for calculating log p. *Journal of Computer-Aided Molecular Design*, 15:337–354, 2001.
- 874 [8] Ashok K Sharma, Gopal N Srivastava, Ankita Roy, and Vineet K Sharma. Toxim: a toxicity  
875 prediction tool for small molecules developed using machine learning and chemoinformatics  
876 approaches. *Frontiers in pharmacology*, 8:880, 2017.
- 877 [9] Rakesh Kanji, Abhinav Sharma, and Ganesh Bagler. Phenotypic side effects prediction by  
878 optimizing correlation with chemical and target profiles of drugs. *Molecular BioSystems*, 11  
879 (11):2900–2906, 2015.
- 880 [10] Brian J Bender, Stefan Gahbauer, Andreas Lutten, Jiankun Lyu, Chase M Webb, Reed M Stein,  
881 Elissa A Fink, Trent E Balius, Jens Carlsson, John J Irwin, et al. A practical guide to large-scale  
882 docking. *Nature protocols*, 16(10):4799–4832, 2021.
- 883 [11] Reed M Stein, Hye Jin Kang, John D McCorvy, Grant C Glatfelter, Anthony J Jones, Tao Che,  
884 Samuel Slocum, Xi-Ping Huang, Olena Savych, Yurii S Moroz, et al. Virtual discovery of  
885 melatonin receptor ligands to modulate circadian rhythms. *Nature*, 579(7800):609–614, 2020.
- 886 [12] Ralf Mueller, Alice L Rodriguez, Eric S Dawson, Mariusz Butkiewicz, Thuy T Nguyen, Stephen  
887 Oleszkiewicz, Annalen Bleckmann, C David Weaver, Craig W Lindsley, P Jeffrey Conn, et al.  
888 Identification of metabotropic glutamate receptor subtype 5 potentiators using virtual high-  
889 throughput screening. *ACS chemical neuroscience*, 1(4):288–305, 2010.
- 890 [13] Liying Zhang, Denis Fourches, Alexander Sedykh, Hao Zhu, Alexander Golbraikh, Sean  
891 Ekins, Julie Clark, Michele C Connelly, Martina Sigal, Dena Hodges, et al. Discovery of  
892 novel antimalarial compounds enabled by qsar-based virtual screening. *Journal of chemical*  
893 *information and modeling*, 53(2):475–492, 2013.
- 894 [14] Bruno J Neves, Rafael F Dantas, Mario R Senger, Cleber C Melo-Filho, Walter CG Valente,  
895 Ana CM de Almeida, João M Rezende-Neto, Elid FC Lima, Ross Paveley, Nicholas Furnham,  
896 et al. Discovery of new anti-schistosomal hits by integration of qsar-based virtual screening and  
897 high content screening. *Journal of medicinal chemistry*, 59(15):7075–7088, 2016.
- 898 [15] Georges E Janssens, Xin-Xuan Lin, Lluís Millan-Ariño, Alan Kavšek, Ilke Sen, Renée I Seinstra,  
899 Nicholas Stroustrup, Ellen AA Nollen, and Christian G Riedel. Transcriptomics-based screening  
900 identifies pharmacological inhibition of hsp90 as a means to defer aging. *Cell Reports*, 27(2):  
901 467–480, 2019.

- 902 [16] Jonathan M Stokes, Kevin Yang, Kyle Swanson, Wengong Jin, Andres Cubillos-Ruiz, Nina M  
903 Donghia, Craig R MacNair, Shawn French, Lindsey A Carfrae, Zohar Bloom-Ackermann, et al.  
904 A deep learning approach to antibiotic discovery. *Cell*, 180(4):688–702, 2020.
- 905 [17] Zhenqin Wu, Bharath Ramsundar, Evan N Feinberg, Joseph Gomes, Caleb Geniesse, Aneesh S  
906 Pappu, Karl Leswing, and Vijay Pande. Moleculenet: a benchmark for molecular machine  
907 learning. *Chemical science*, 9(2):513–530, 2018.
- 908 [18] Kexin Huang, Tianfan Fu, Wenhao Gao, Yue Zhao, Yusuf Roohani, Jure Leskovec, Connor W  
909 Coley, Cao Xiao, Jimeng Sun, and Marinka Zitnik. Therapeutics data commons: Machine learn-  
910 ing datasets and tasks for drug discovery and development. *arXiv preprint arXiv:2102.09548*,  
911 2021.
- 912 [19] Arash Keshavarzi Arshadi, Milad Salem, Arash Firouzbakht, and Jiann Shiun Yuan. Moldata, a  
913 molecular benchmark for disease and target based machine learning. *Journal of Cheminformatics*,  
914 14(1):1–18, 2022.
- 915 [20] Yuanfeng Ji, Lu Zhang, Jiayang Wu, Bingzhe Wu, Long-Kai Huang, Tingyang Xu, Yu Rong,  
916 Lanqing Li, Jie Ren, Ding Xue, et al. Drugood: Out-of-distribution (ood) dataset curator and  
917 benchmark for ai-aided drug discovery—a focus on affinity prediction problems with noise  
918 annotations. *arXiv preprint arXiv:2201.09637*, 2022.
- 919 [21] Shurui Gui, Xiner Li, Limei Wang, and Shuiwang Ji. Good: A graph out-of-distribution  
920 benchmark. *arXiv preprint arXiv:2206.08452*, 2022.
- 921 [22] Ziqiao Zhang, Bangyi Zhao, Ailin Xie, Yatao Bian, and Shuigeng Zhou. Activity cliff prediction:  
922 Dataset and benchmark. *arXiv preprint arXiv:2302.07541*, 2023.
- 923 [23] Derek van Tilborg, Alisa Alenicheva, and Francesca Grisoni. Exposing the limitations of  
924 molecular machine learning with activity cliffs. *Journal of Chemical Information and Modeling*,  
925 62(23):5938–5951, 2022.
- 926 [24] György M Keserű and Gergely M Makara. Hit discovery and hit-to-lead approaches. *Drug*  
927 *discovery today*, 11(15-16):741–748, 2006.
- 928 [25] Asher Mullard. How much do phase iii trials cost? *Nature Reviews. Drug Discovery*, 17(11):  
929 777–777, 2018.
- 930 [26] Linda Martin, Melissa Hutchens, Conrad Hawkins, and Alaina Radnov. How much do clinical  
931 trials cost. *Nat Rev Drug Discov*, 16(6):381–382, 2017.
- 932 [27] Jiankun Lyu, Sheng Wang, Trent E Balius, Isha Singh, Anat Levit, Yurii S Moroz, Matthew J  
933 O’Meara, Tao Che, Enkhjargal Alгаа, Kateryna Tolmachova, et al. Ultra-large library docking  
934 for discovering new chemotypes. *Nature*, 566(7743):224–229, 2019.
- 935 [28] Felix Wong, Satotaka Omori, Nina M Donghia, Erica J Zheng, and James J Collins. Discovering  
936 small-molecule senolytics with deep neural networks. *Nature Aging*, pages 1–17, 2023.
- 937 [29] Gary Liu, Denise B Catacutan, Khushi Rathod, Kyle Swanson, Wengong Jin, Jody C Mo-  
938 hammed, Anush Chiappino-Pepe, Saad A Syed, Meghan Fraxis, Kenneth Rachwalski, et al.  
939 Deep learning-guided discovery of an antibiotic targeting acinetobacter baumannii. *Nature*  
940 *Chemical Biology*, pages 1–9, 2023.
- 941 [30] RD Brown and YC Martin. An evaluation of structural descriptors and clustering methods for  
942 use in diversity selection. *SAR and QSAR in Environmental Research*, 8(1-2):23–39, 1998.
- 943 [31] Bie Verbist, Günter Klambauer, Liesbet Vervoort, Willem Talloen, Ziv Shkedy, Olivier Thas,  
944 Andreas Bender, Hinrich WH Göhlmann, Sepp Hochreiter, QSTAR Consortium, et al. Using  
945 transcriptomics to guide lead optimization in drug discovery projects: Lessons learned from the  
946 qstar project. *Drug discovery today*, 20(5):505–513, 2015.

- 947 [32] George Papadatos, Anthony WJ Cooper, Visakan Kadirkamanathan, Simon JF Macdonald,  
948 Iain M McLay, Stephen D Pickett, John M Pritchard, Peter Willett, and Valerie J Gillet. Analysis  
949 of neighborhood behavior in lead optimization and array design. *Journal of chemical information  
950 and modeling*, 49(2):195–208, 2009.
- 951 [33] Nathan Brown, Marco Fiscato, Marwin HS Segler, and Alain C Vaucher. Guacamol: bench-  
952 marking models for de novo molecular design. *Journal of chemical information and modeling*,  
953 59(3):1096–1108, 2019.
- 954 [34] Tianfan Fu, Cao Xiao, Xinhao Li, Lucas M Glass, and Jimeng Sun. Mimoso: Multi-constraint  
955 molecule sampling for molecule optimization. In *Proceedings of the AAAI Conference on  
956 Artificial Intelligence*, volume 35, pages 125–133, 2021.
- 957 [35] Wengong Jin, Regina Barzilay, and Tommi Jaakkola. Junction tree variational autoencoder for  
958 molecular graph generation. In *International conference on machine learning*, pages 2323–2332.  
959 PMLR, 2018.
- 960 [36] Maxime Langevin, Hervé Minoux, Maximilien Levesque, and Marc Bianciotto. Scaffold-  
961 constrained molecular generation. *Journal of Chemical Information and Modeling*, 60(12):  
962 5637–5646, 2020.
- 963 [37] William J Godinez, Eric J Ma, Alexander T Chao, Luying Pei, Peter Skewes-Cox, Stephen M  
964 Canham, Jeremy L Jenkins, Joseph M Young, Eric J Martin, and W Armand Guiguemde. Design  
965 of potent antimalarials with generative chemistry. *Nature Machine Intelligence*, 4(2):180–186,  
966 2022.
- 967 [38] Wenhao Gao, Tianfan Fu, Jimeng Sun, and Connor Coley. Sample efficiency matters: a  
968 benchmark for practical molecular optimization. *Advances in Neural Information Processing  
969 Systems*, 35:21342–21357, 2022.
- 970 [39] David E Patterson, Richard D Cramer, Allan M Ferguson, Robert D Clark, and Laurence E  
971 Weinberger. Neighborhood behavior: a useful concept for validation of “molecular diversity”  
972 descriptors. *Journal of medicinal chemistry*, 39(16):3049–3059, 1996.
- 973 [40] Yvonne C Martin, James L Kofron, and Linda M Traphagen. Do structurally similar molecules  
974 have similar biological activity? *Journal of medicinal chemistry*, 45(19):4350–4358, 2002.
- 975 [41] Gerald Maggiora, Martin Vogt, Dagmar Stumpfe, and Jurgen Bajorath. Molecular similarity in  
976 medicinal chemistry: miniperspective. *Journal of medicinal chemistry*, 57(8):3186–3204, 2014.
- 977 [42] Alex Zhavoronkov and Alán Aspuru-Guzik. Reply to ‘assessing the impact of generative ai on  
978 medicinal chemistry’. *Nature Biotechnology*, 38(2):146–146, 2020.
- 979 [43] Pedro Franco, Nuria Porta, John D Holliday, and Peter Willett. The use of 2d fingerprint  
980 methods to support the assessment of structural similarity in orphan drug legislation. *Journal of  
981 cheminformatics*, 6:1–10, 2014.
- 982 [44] David Rogers and Mathew Hahn. Extended-connectivity fingerprints. *Journal of chemical  
983 information and modeling*, 50(5):742–754, 2010.
- 984 [45] John D Holliday, Naomie Salim, Martin Whittle, and Peter Willett. Analysis and display of  
985 the size dependence of chemical similarity coefficients. *Journal of chemical information and  
986 computer sciences*, 43(3):819–828, 2003.
- 987 [46] Wei Lu, Qifeng Wu, Jixian Zhang, Jiahua Rao, Chengtao Li, and Shuangjia Zheng. Tankbind:  
988 Trigonometry-aware neural networks for drug-protein binding structure prediction. *bioRxiv*,  
989 pages 2022–06, 2022.

- 990 [47] Seul Lee, Jaehyeong Jo, and Sung Ju Hwang. Exploring chemical space with score-based out-of-  
991 distribution generation. In *International Conference on Machine Learning*, pages 18872–18892.  
992 PMLR, 2023.
- 993 [48] Hyeoncheol Cho and Insung S Choi. Enhanced deep-learning prediction of molecular properties  
994 via augmentation of bond topology. *ChemMedChem*, 14(17):1604–1609, 2019.
- 995 [49] Yoonho Jeong, Jihoo Kim, Yeji Kim, and Insung S Choi. Development of a chemically intuitive  
996 filter for chemical graph convolutional network. *Bulletin of the Korean Chemical Society*, 43(7):  
997 934–936, 2022.
- 998 [50] Benson Chen, Regina Barzilay, and Tommi Jaakkola. Path-augmented graph transformer  
999 network. *arXiv preprint arXiv:1905.12712*, 2019.
- 1000 [51] Prateeth Nayak, Andrew Silberfarb, Ran Chen, Tulay Muezzinoglu, and John Byrnes. Trans-  
1001 former based molecule encoding for property prediction. *arXiv preprint arXiv:2011.03518*,  
1002 2020.
- 1003 [52] Ross Irwin, Spyridon Dimitriadis, Jiazhen He, and Esben Jannik Bjerrum. Chemformer: a pre-  
1004 trained transformer for computational chemistry. *Machine Learning: Science and Technology*,  
1005 3(1):015022, 2022.
- 1006 [53] Yao Zhang et al. Bayesian semi-supervised learning for uncertainty-calibrated prediction of  
1007 molecular properties and active learning. *Chemical science*, 10(35):8154–8163, 2019.
- 1008 [54] Guy W Bemis and Mark A Murcko. The properties of known drugs. 1. molecular frameworks.  
1009 *Journal of medicinal chemistry*, 39(15):2887–2893, 1996.
- 1010 [55] Bihter Das, Mucahit Kutsal, and Resul Das. Effective prediction of drug–target interaction on  
1011 hiv using deep graph neural networks. *Chemometrics and Intelligent Laboratory Systems*, 230:  
1012 104676, 2022.
- 1013 [56] Garrett B Goh, Charles M Siegel, Abhinav Vishnu, and Nathan O Hodas. Chemnet: A  
1014 transferable and generalizable deep neural network for small-molecule property prediction.  
1015 Technical report, Pacific Northwest National Lab.(PNNL), Richland, WA (United States), 2017.
- 1016 [57] Shion Honda, Shoi Shi, and Hiroki R Ueda. Smiles transformer: Pre-trained molecular  
1017 fingerprint for low data drug discovery. *arXiv preprint arXiv:1911.04738*, 2019.
- 1018 [58] Chao Shang, Qinqing Liu, Ko-Shin Chen, Jiangwen Sun, Jin Lu, Jinfeng Yi, and Jinbo Bi.  
1019 Edge attention-based multi-relational graph convolutional networks. *arXiv preprint arXiv:*  
1020 *1802.04944*, 2018.
- 1021 [59] Karim Abbasi, Antti Poso, Jahanbakhsh Ghasemi, Massoud Amanlou, and Ali Masoudi-  
1022 Nejad. Deep transferable compound representation across domains and tasks for low data drug  
1023 discovery. *Journal of chemical information and modeling*, 59(11):4528–4539, 2019.
- 1024 [60] Dilyana Dimova and Jürgen Bajorath. Advances in activity cliff research. *Molecular informatics*,  
1025 35(5):181–191, 2016.
- 1026 [61] Denis Cornaz, Fabio Furini, Mathieu Lacroix, Enrico Malaguti, A Ridha Mahjoub, and Sébastien  
1027 Martin. Mathematical formulations for the balanced vertex k-separator problem. In *2014*  
1028 *International Conference on Control, Decision and Information Technologies (CoDIT)*, pages  
1029 176–181. IEEE, 2014.
- 1030 [62] Egon Balas and Cid C de Souza. The vertex separator problem: a polyhedral investigation.  
1031 *Mathematical Programming*, 103(3):583–608, 2005.
- 1032 [63] Stephan Schwartz. An overview of graph covering and partitioning. *Discrete Mathematics*, 345  
1033 (8):112884, 2022.

- 1034 [64] Denis Cornaz, Fabio Furini, Mathieu Lacroix, Enrico Malaguti, A Ridha Mahjoub, and Sébastien  
1035 Martin. The vertex  $k$ -cut problem. *Discrete Optimization*, 31:8–28, 2019.
- 1036 [65] Paolo Paronuzzi. Models and algorithms for decomposition problems. 2020.
- 1037 [66] Fabio Furini, Ivana Ljubić, Enrico Malaguti, and Paolo Paronuzzi. On integer and bilevel  
1038 formulations for the  $k$ -vertex cut problem. *Mathematical Programming Computation*, 12:  
1039 133–164, 2020.
- 1040 [67] Yangming Zhou, Gezi Wang, and MengChu Zhou. Detecting  $k$ -vertex cuts in sparse networks  
1041 via a fast local search approach. *IEEE Transactions on Computational Social Systems*, 2023.
- 1042 [68] Darko Butina. Unsupervised data base clustering based on daylight’s fingerprint and tanimoto  
1043 similarity: A fast and automated way to cluster small and large data sets. *Journal of Chemical  
1044 Information and Computer Sciences*, 39(4):747–750, 1999.
- 1045 [69] Yutong Xie, Ziqiao Xu, Jiaqi Ma, and Qiaozhu Mei. How much space has been explored?  
1046 measuring the chemical space covered by databases and machine-generated molecules. In *The  
1047 Eleventh International Conference on Learning Representations*.
- 1048 [70] Thelma Beatriz González-Castro, Yazmin Hernandez-Diaz, Isela Esther Juárez-Rojop,  
1049 María Lilia López-Narváez, Carlos Alfonso Tovilla-Zárate, Alma Genis-Mendoza, and Mariela  
1050 Alpuin-Reyes. The role of c957t, taqi and ser311cys polymorphisms of the drd2 gene in  
1051 schizophrenia: systematic review and meta-analysis. *Behavioral and Brain Functions*, 12(1):  
1052 1–14, 2016.
- 1053 [71] Ritushree Kukreti, Sudipta Tripathi, Pallav Bhatnagar, Simone Gupta, Chitra Chauhan, Shob-  
1054 hana Kubendran, YC Janardhan Reddy, Sanjeev Jain, and Samir K Brahmachari. Association  
1055 of drd2 gene variant with schizophrenia. *Neuroscience letters*, 392(1-2):68–71, 2006.
- 1056 [72] V McGuire, SK Van Den Eeden, CM Tanner, F Kamel, DM Umbach, K Marder, R Mayeux,  
1057 B Ritz, GW Ross, H Petrovitch, et al. Association of drd2 and drd3 polymorphisms with  
1058 parkinson’s disease in a multiethnic consortium. *Journal of the neurological sciences*, 307(1-2):  
1059 22–29, 2011.
- 1060 [73] Dongjun Dai, Yunliang Wang, Lingyan Wang, Jinfeng Li, Qingqing Ma, Jianmin Tao, Xingyu  
1061 Zhou, Hanlin Zhou, Yi Jiang, Guanghui Pan, et al. Polymorphisms of drd2 and drd3 genes and  
1062 parkinson’s disease: A meta-analysis. *Biomedical reports*, 2(2):275–281, 2014.
- 1063 [74] David Mendez, Anna Gaulton, A Patrícia Bento, Jon Chambers, Marleen De Veij, Eloy Félix,  
1064 María Paula Magariños, Juan F Mosquera, Prudence Mutowo, Michał Nowotka, et al. ChEMBL:  
1065 towards direct deposition of bioassay data. *Nucleic acids research*, 47(D1):D930–D940, 2019.
- 1066 [75] Siddharth J Modi and Vithal M Kulkarni. Vascular endothelial growth factor receptor (vegfr-  
1067 2)/kdr inhibitors: medicinal chemistry perspective. *Medicine in Drug Discovery*, 2:100009,  
1068 2019.
- 1069 [76] Cheng Fang, Ye Wang, Richard Grater, Sudarshan Kapadnis, Cheryl Black, Patrick Trapa,  
1070 and Simone Sciabola. Prospective validation of machine learning algorithms for absorption,  
1071 distribution, metabolism, and excretion prediction: An industrial perspective. *Journal of  
1072 Chemical Information and Modeling*, 2023.
- 1073 [77] Takaya Saito and Marc Rehmsmeier. The precision-recall plot is more informative than the  
1074 roc plot when evaluating binary classifiers on imbalanced datasets. *PloS one*, 10(3):e0118432,  
1075 2015.
- 1076 [78] Kelly Rae Chi. Revolution dawning in cardiotoxicity testing. *Nature reviews. Drug discovery*,  
1077 12(8):565, 2013.

- 1078 [79] Kevin Yang, Kyle Swanson, Wengong Jin, Connor Coley, Philipp Eiden, Hua Gao, Angel  
1079 Guzman-Perez, Timothy Hopper, Brian Kelley, Miriam Mathea, et al. Analyzing learned molec-  
1080 ular representations for property prediction. *Journal of chemical information and modeling*, 59  
1081 (8):3370–3388, 2019.
- 1082 [80] Yu Shi, Shuxin Zheng, Guolin Ke, Yifei Shen, Jiacheng You, Jiyan He, Shengjie Luo, Chang Liu,  
1083 Di He, and Tie-Yan Liu. Benchmarking graphormer on large-scale molecular modeling datasets.  
1084 *arXiv preprint arXiv:2203.04810*, 2022. URL <https://arxiv.org/abs/2203.04810>.
- 1085 [81] Chengxuan Ying, Tianle Cai, Shengjie Luo, Shuxin Zheng, Guolin Ke, Di He, Yanming Shen,  
1086 and Tie-Yan Liu. Do transformers really perform badly for graph representation? In *Thirty-Fifth*  
1087 *Conference on Neural Information Processing Systems*, 2021. URL [https://openreview.](https://openreview.net/forum?id=0eWoo0xFwDa)  
1088 [net/forum?id=0eWoo0xFwDa](https://openreview.net/forum?id=0eWoo0xFwDa).
- 1089 [82] Joelle Pineau, Philippe Vincent-Lamarre, Koustuv Sinha, Vincent Larivière, Alina Beygelzimer,  
1090 Florence d’Alché Buc, Emily Fox, and Hugo Larochelle. Improving reproducibility in machine  
1091 learning research (a report from the neurips 2019 reproducibility program). *The Journal of*  
1092 *Machine Learning Research*, 22(1):7459–7478, 2021.
- 1093 [83] Mario Lucic, Karol Kurach, Marcin Michalski, Sylvain Gelly, and Olivier Bousquet. Are gans  
1094 created equal? a large-scale study. *Advances in neural information processing systems*, 31,  
1095 2018.
- 1096 [84] Gábor Melis, Chris Dyer, and Phil Blunsom. On the state of the art of evaluation in neural  
1097 language models. *arXiv preprint arXiv:1707.05589*, 2017.
- 1098 [85] Megan Stanley, John F Bronskill, Krzysztof Maziarz, Hubert Misztela, Jessica Lanini, Marwin  
1099 Segler, Nadine Schneider, and Marc Brockschmidt. Fs-mol: A few-shot learning dataset of  
1100 molecules. In *Thirty-fifth Conference on Neural Information Processing Systems Datasets and*  
1101 *Benchmarks Track (Round 2)*, 2021.
- 1102 [86] Zaixi Zhang and Qi Liu. Learning subpocket prototypes for generalizable structure-based drug  
1103 design. *arXiv preprint arXiv:2305.13997*, 2023.
- 1104 [87] Tuomo Kalliokoski, Christian Kramer, Anna Vulpetti, and Peter Gedeck. Comparability of  
1105 mixed ic50 data—a statistical analysis. *PloS one*, 8(4):e61007, 2013.
- 1106 [88] Christian Kramer, Tuomo Kalliokoski, Peter Gedeck, and Anna Vulpetti. The experimental  
1107 uncertainty of heterogeneous public k i data. *Journal of medicinal chemistry*, 55(11):5165–5173,  
1108 2012.